Bioorg. Med. Chem. 94 (2023) 117438

Contents lists available at ScienceDirect

Bioorganic & Medicinal Chemistry

journal homepage: www.elsevier.com/locate/bmc

DNA major versus minor groove occupancy of monomeric and dimeric crystal violet derivatives. Toward structural correlations

Aren Mirzakhanian, Michael Khoury, Donald E. Trujillo, Byoula Kim, Donnie Ca, Thomas Minehan *

Department of Chemistry and Biochemistry, California State University, Northridge, 18111 Nordhoff Street, Northridge, CA 91330, USA

ARTICLE INFO

Keywords:
Triphenylmethane dyes
Nucleic acids
Major groove
Stereoelectronic interactions
Molecular docking

ABSTRACT

Six monomeric (1a-1f) and five dimeric (2a-2e) derivatives of the triphenylmethane dye crystal violet (CV) have been prepared. Evaluation of the binding of these compounds to CT DNA by competitive fluorescent intercalator displacement (FID) assays, viscosity experiments, and UV and CD spectroscopy suggest that monomeric derivative 1a and dimeric derivative 2d likely associate with the major groove of DNA, while dimeric derivatives 2a and 2e likely associate with the minor groove of DNA. Additional evidence for the groove occupancy assignments of these derivatives was obtained from ITC experiments and from differential inhibition of DNA cleavage by the major groove binding restriction enzyme *Bam*HI, as revealed by agarose gel electrophoresis. The data indicate that major groove ligands may be optimally constructed from dye units containing a sterically bulky 3,5-dimethyl-*N,N*-dimethylaniline group; furthermore, the groove-selectivity of olefin-tethered dimer 2d suggests that stereoelectronic interactions (n → π*) between the ligand and DNA are also an important design consideration in the crafting of major-groove binding ligands.

1. Introduction

Major groove binding small molecules which can directly compete with transcription factors and other DNA binding proteins for their cognate sites on DNA have the potential to regulate gene expression.[1] However, relatively few naturally-ocurring substances associate with the major groove of DNA.[2a] The majority of nucleic acid-binding natural products prefer to occupy the narrower minor groove, where hydrophobic and van der Waals interactions with the walls and floor of the groove are maximized.[2b] Non-natural major groove binders have also been developed, such as ditercalinium,[3] Iverson's naphthalene-diimide peptides,[4] and Arya's neomycin-neomycin dimer[5]. More recently, Berdnikova demonstrated that mono- and bis-styryl dyes possessing an oxodecyl chain preferentially occupy the major groove of DNA.[6] Furthermore, Mollica has shown that β-hairpin peptides and β-sheet analogs of the ARC protein bind the major groove with modest sequence selectivities.[7] The cationic triphenylmethane dyes crystal violet (CV) and methyl green (MG) are histochemical stains known to bind duplex DNA by a non-intercalative mode of association.[8] Evidence presented by Kim and Norden[8d] suggests that methyl green binds the major groove of DNA. Motivated by these findings, we previously prepared dimeric and trimeric derivatives of crystal violet (CV) that displayed submicromolar affinities for duplex DNA; furthermore, competitive DNA binding studies and CD spectroscopy provided evidence that the tightest binding trimeric derivative most likely associates with the major groove of DNA, with an approximately 10-fold preference for binding AT-rich homopolymers over GC-rich sequences.[9] It has been shown by Arya that sterically bulky major groove ligands prefer to bind the wider major groove of non-alternating AT-rich DNA (termed B*-form DNA)[5b] over typical B-form DNA.[5] To further probe ligand structural factors important for major versus minor groove binding, we designed a series of six monomeric CV derivatives (Figure 1) with varying degress of steric bulk, containing two (**1a**) or three (**1b**) methyl groups and one (**1d**), two (**1e**), or three (**1f**) phenyl groups on the aromatic rings of the dye, as well as an expanded dye possessing a naphthyl group (**1c**). In addition, five dimeric CV derivatives (Figure 2) were designed with dye units connected to an *ortho*-substituted aryl core by *ortho* or *para*-aryl (**2a**, **2b**), alkynyl (**2c**), alkenyl (**2d**), or alkoxyalkyl (**2e**) linkers. The benzodioxole core employed for derivatives **2b**, **2c,** and **2d** enhanced the stability of the dyes through resonance interaction of the oxygen lone pairs with the triphenylmethane carbocations, as also observed in dimer **2e**; the less stable but more compact compound **2a** with a phenyl core was prepared

* Corresponding author.
E-mail address: thomas.minehan@csun.edu (T. Minehan).

https://doi.org/10.1016/j.bmc.2023.117438
Received 22 May 2023; Received in revised form 5 August 2023; Accepted 7 August 2023
Available online 11 August 2023

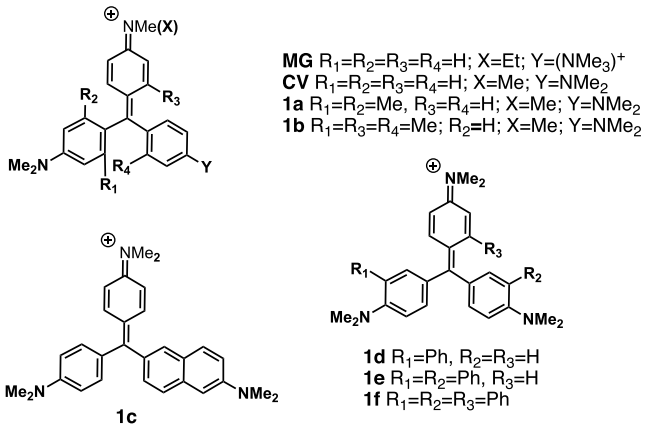

Figure 1. Structures of the cationic dyes methyl green (MG), crystal violet (CV) and synthetic derivatives **1a**-**1f**.

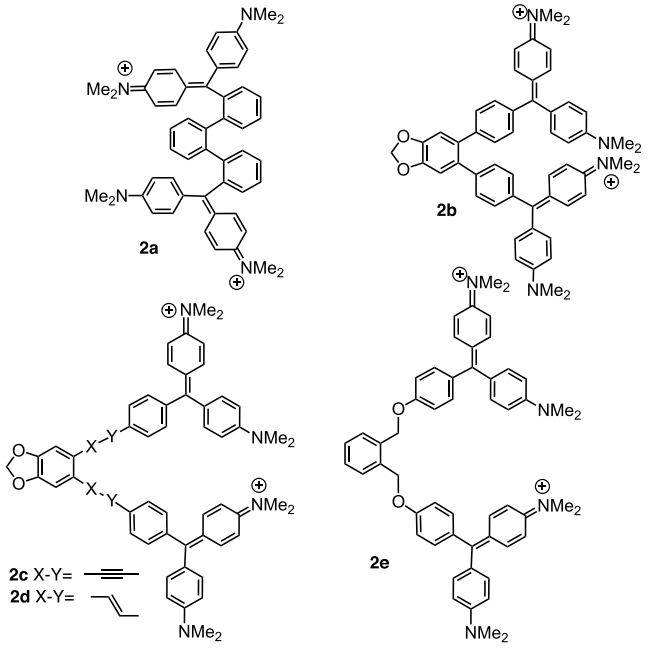

Figure 2. Structures of synthetic CV derivatives **2a**-**2e**.

because of low yields encountered in the starting material synthesis with 5,6-dibromo-1,3-benzodioxole. We envisioned that the sp, sp^2, and sp^3-hybridized linkers in compounds **2c**, **2d**, and **2e**, respectively, would allow an assessment of the impact of extended charge delocalization from the peripheral dye units on ligand-DNA binding. The synthetic pathways to these compounds, as well as analyses of their DNA binding mode and sequence selectivity, are detailed herein.

2. Results and discussion

2.1. Chemistry

A slight modification of a reported protocol for the synthesis of triphenylmethane dyes[10] was followed to prepare compounds **1a**-**1f**. Three equivalents of 3-methyl-4-bromo-*N,N*-dimethylaniline was treated with *n*-BuLi (THF, 78 °C), and in 10 min ethyl-2-methyl-4-dimethylamino-benzoate was added; after stirring for 3 h at room temperature, aqueous acidic workup and purification afforded compound **1b** in 70% yield (Scheme 1). It was found that silica gel chromatography of the dye products resulted in very low (20%) isolated

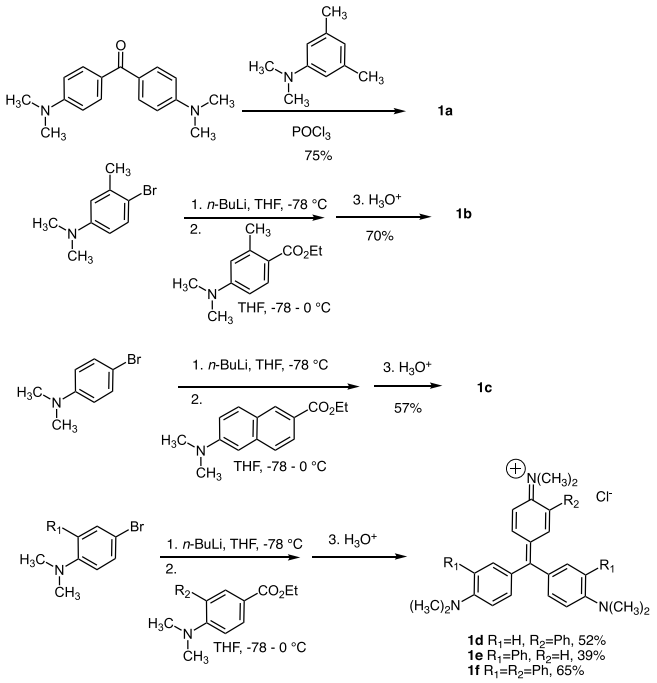

Scheme 1. Synthesis of ligands **1a**-**1f**.

yields, a problem that was ultimately circumvented by switching to size-exclusion chromatography using Sephadex LH-20. Reaction of 4-bromo-*N,N*-dimethylaniline and ethyl-6-(dimethylamino)-2-naphthalene-carboxylate gave **1c** in 57% yield. Further, compounds **1d**, **1e**, and **1f** were prepared in 52%, 39%, and 65% yields, respectively, by an analogous reaction sequence from either 4-bromo-*N,N*-dimethylaniline or 2-phenyl-4-bromo-*N,N*-dimethylaniline and either ethyl-4-dimethyl-aminobenzoate or ethyl-3-phenyl-4-dimethylaminobenzoate. Finally, ligand **1a** was prepared in 75% isolated yield following the protocol of Barker, Bride, and Stamp[11] in which *N,N*-3,5-tetramethylaniline was heated with Mischler's ketone in $POCl_3$ for 5 h at 100 °C, followed by aqueous workup and purification.

For the preparation of dimeric CV derivatives, a protocol involving combination of excess aryllithium reagent with various diesters was employed (see Supporting Information File). Thus, the reaction of five equiv of 4-lithio-*N,N*-dimethylaniline (obtained by treatment of 4-bromo-*N,N*-dimethylaniline with 1.1 equiv of *n*-BuLi in THF at 78 °C) with 1 equiv of diester, followed by warming to rt and aqueous acidic workup and purification, gave compounds **2a**, **2b**, **2c**, **2d** and **2e** in 43%, 63%, 53%, 40% and 61% yields, respectively (Scheme 2).

2.2. DNA binding evaluation

To evaluate the ability of these eleven compounds to recognize CT DNA, we performed competitive ethidium displacement assays[12] in the presence and absence of the minor groove binder netropsin or the major groove binder methyl green, and compared C_{50} values (the concentration of ligand required to achieve a 50% decrease in the fluorescence of ethidium bromide, Figure 3 a,b) and apparent binding affinities (K_{app} = 9.5 × 10^6 M ^{1} × $C_{ethidium}/C_{50}$, Table 1a). The tightest binding monomeric CV derivative is **1e** (K_{app} = 21.6 ± 0.1 × 10^6 M ^{1}) containing two phenyl groups attached to the triphenylmethane core. Comparing K_{app} values in the presence of netropsin or methyl green, it is apparent that compound **1a** (K_{app} = 9.5 ± 0.4 × 10^6 M ^{1}) provides the most compelling evidence for major groove occupancy, with a > 8-fold lower K_{app} value (1.1 ± 0.1 × 10^6 M ^{1}) recorded in the presence of methyl green, versus only a 1.3-fold lower value (7.5 ± 0.1 × 10^6 M ^{1}) in the presence of netropsin. Further, compound **1d** (K_{app} = 1.63 ± 0.02 × 10^6

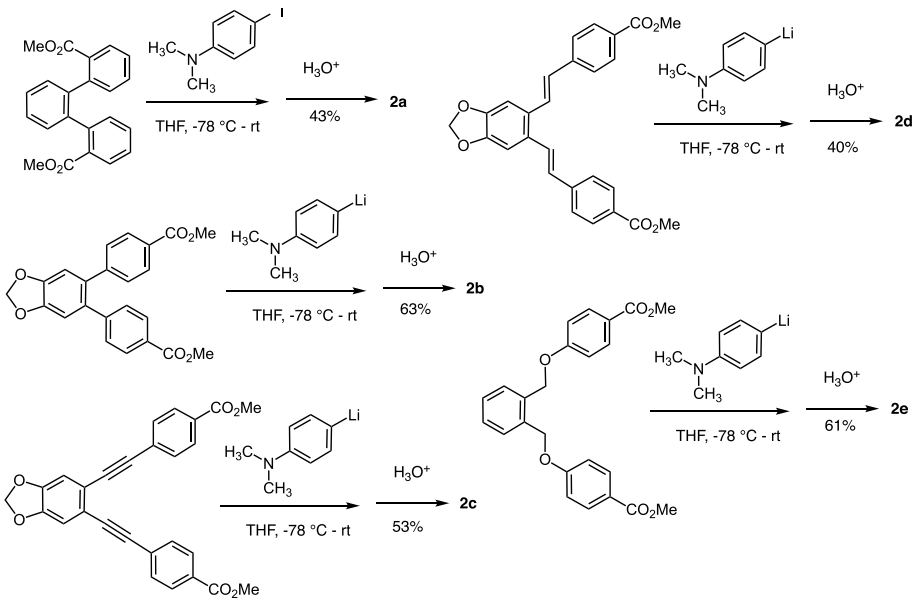

Scheme 2. Synthesis of ligands **2a-2e**.

M ^{1}) displayed a 5-fold lower K_{app} value in the presence of methyl green ($0.72 \pm 0.01 \times 10^{6}$ M ^{1}) versus in the presence of netropsin ($3.54 \pm 0.16 \times 10^{6}$ M ^{1}), an observation again suggestive of major groove occupancy. In contrast, compounds **1b**, **1c**, **1e**, and **1f** showed no strong preference for major or minor groove binding from competitive inhibition analysis. For CV derivatives **2a-2e**, the tightest binding compound was **2a** ($K_{app} = 95 \pm 1.9 \times 10^{6}$ M ^{1}), which together with derivative **2e** ($K_{app} = 33 \pm 2.2 \times 10^{6}$ M ^{1}) evidenced minor groove binding by displaying lower K_{app} values in the presence of netropsin ($K_{app} = 62.5 \pm 2.4 \times 10^{6}$ M ^{1} and $9.5 \pm 0.2 \times 10^{6}$ M ^{1} for **2a** and **2e**, respectively) versus in the presence of methyl green ($K_{app} = 81.9 \pm 2.2 \times 10^{6}$ M ^{1} and $16.0 \pm 1.0 \times 10^{6}$ M ^{1} for **2a** and **2e**, respectively). Compound **2d** ($K_{app} = 37.0 \pm 2.8 \times 10^{6}$ M ^{1}) showed a strong preference for major groove binding, displaying a > 8-fold lower apparent affinity for CT DNA in the presence of methyl green ($K_{app} = 4.4 \pm 1.3 \times 10^{6}$ M ^{1}) versus in the presence or absence of netropsin ($K_{app} \sim 37 \pm 3.0 \times 10^{6}$ M ^{1}). Compound **2c** evidences a mixed binding mode, while compound **2b** displays a preference for major groove binding. *K* values derived from ITC titrations of **1a-1f** and **2a-2e** with the DDD hairpin (Figure 8b) are provided for comparison in Table 1b.

Monitoring the titrations of compounds **1a**, **2a**, **2d**, and **2e** with CT DNA by UV spectroscopy[29] revealed hypochromic and bathochromic shifts in the main dye absorption bands centered around 375–450 nm and 600–620 nm (see Figure 4a and Supporting Information file). Such shifts have been observed for both intercalating and groove binding compounds.[13] To verify that the dye derivatives are groove binders and not intercalators, we performed CT DNA solution viscosity experiments with compounds **1a**, **2a**, **2d** and **2e**. The lengthening and rigidification of DNA that results from intercalation of drugs between the base-pair stack has been shown to give rise to an increase in solution viscosity.[14] Figure 4b shows a plot of the relative viscosities of intercalator control compound ethidium bromide and **1a** versus the ligand/DNA ratio. Whereas increasing concentrations of ethidium bromide increases the viscosity of the CT DNA solution, increasing concentrations of **1a** show minimal changes in CT DNA solution viscosity over the concentration range studied. Similar results were obtained for compound **2a** as well as control compound methyl green. However, increasing concentrations of the larger dyes **2d** and **2e** showed a slight *decrease* in CT DNA solution viscosity. A decrease in solution viscosity may result from a groove binding mode that induces DNA bending. [32]

Data from circular dichroism experiments provided additional support for the groove occupancy assignments of **1a**, **1d**, **2a**, **2d**, and **2e**. Wilson et al.[15a] have reported that titrations of DNA with groove binders produce positive induced CD (ICD) bands, while Garoufis[15b] and Hannon[15c] have indicated the development of negative ICD bands. To establish a reference point for our system, we observed that titration of CT DNA with the structurally similar major groove binding dye methyl green results in a strong negative induced CD band (ICD) at 310 nm (see Supporting Information file). Repetition of the CD experiments with a DNA hairpin containing the Drew-Dickerson dodecamer (DDD) sequence (Figure 8b)[25] yielded very similar results to those obtained with CT DNA. As can be seen in Figures 5a and 5b, CD titrations of the DDD hairpin with compounds **1a** and **2d** both produce negative ICD bands at ~ 310 nm (a similar profile was observed for titration of CT DNA with **1d**), corresponding to the UV absorption of the bound dye at the same wavelength.[15] Furthermore, although titrations of **2d** with the DDD oligo show a strong decrease in the base stacking band (280 nm) at higher **2d**:DNA ratios, negligible changes in the helicity band at 245 nm are observed over the same concentration range, an observation inconsistent with intercalative binding.[16a]

In contrast, CD spectra of titrations of CT DNA with **2a** and **2e** showed positive ICD bands above 300 nm (Figure 5 c,f).[16b] The bisignate nature of the 335 nm ICD band of **2e** may be indicative of dye aggregation in the DNA groove;[6] in addition, two new absorptions at 310 and 337 nm observed in UV spectral titrations of **2e** with CT DNA, attributable to the bound (DNA-dye) complex, lend support to this hypothesis.

ITC titrations[17] of CT DNA (100 μM/bp) with compounds **1a**, **2d**, and **2e** (100 μM solutions, 25 °C, pH = 7.0, 10 mM Tris-HCl buffer) provided thermodynamic data also suggestive of differential groove occupancy.[17e] Whereas the binding of compound **2e** is clearly enthalpy driven (ΔH = -44.7 kcal/mol, ΔS = -120 cal/mol•K, Figure 6), the data for both **1a** and **2d** clearly indicate an entropy-driven process (ΔH = 29.7 kcal/mol, ΔS = 122 cal/mol•K for **1a**, Figure 6; ΔH = 85.8 kcal/mol, ΔS = 316 cal/mol•K for **2d**). A strong entropic contribution to the binding free energy is characteristic of agents that associate with the major groove of DNA due to the release of bound water molecules to bulk solvent upon binding.[18]

To obtain additional support for the DNA binding mode of the synthetic CV derivatives, we examined cleavage of pUC-19 plasmid DNA by the major-groove binding restriction enzyme BamH1 (5′-GˆGATCC-3′)[19] in the presence of the major and minor-groove binding small molecules methyl green and netropsin, respectively.[30] Whereas the concentration

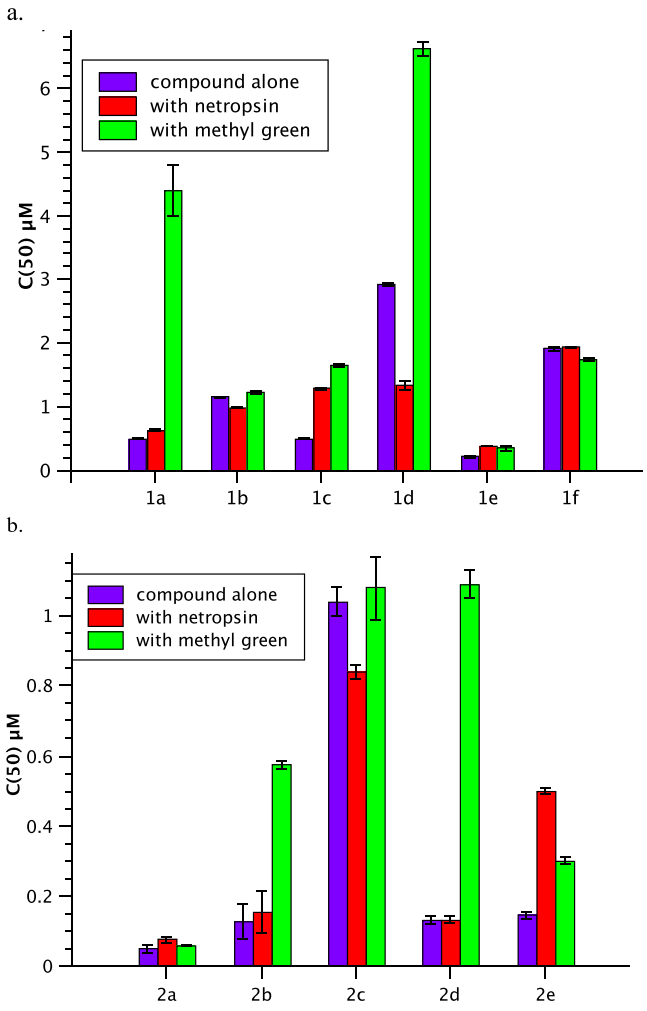

Figure 3. (a) C_{50} values (in μM) for the binding of compounds **1a-1f** to CT DNA (0.625 μM/bp, + 5 μM ethidium bromide, 10 mM Tris-HCl, pH = 7.0) in the absence (blue bar) or presence of netropsin (2.0 μM, red bar) or methyl green (2 μM, green bar). (b) C_{50} values (in μM) for the binding of compounds **2a-2e** to CT DNA (1.0 μM/bp, + 0.5 μM ethidium bromide, 10 mM Tris-HCl, pH = 7.0) in the absence (blue bar) or presence of netropsin (0.5 μM, red bar) or methyl green (0.5 μM, green bar). Error bars represent the standard deviation of three replicate experiments. (For interpretation of the references to colour in this figure legend, the reader is referred to the web version of this article.)

Table 1a
K_{app}, r_{bd}, and ΔT_m values for the binding of **1a-1f** and **2a-2e** to CT DNA in the presence or absence of netropsin or methyl green.

	K_{app} [a]/K ($\times 10^6$ M $^{-1}$)	r_{bd} [b]	ΔT_M [c] (°C)	K_{app} + netropsin [d] ($\times 10^6$ M $^{-1}$)	K_{app} + methyl green [d] ($\times 10^6$ M $^{-1}$)
1a	**9.5 ± 0.4**	**2.2**	**2.8**	**7.5 ± 0.1**	**1.1 ± 0.1**
1b	4.10 ± 0.07	2.3	2.6	4.79 ± 0.10	3.86 ± 0.06
1c	9.5 ± 0.2	3.1	4.6	3.68 ± 0.03	2.87 ± 0.06
1d	1.63 ± 0.02	1.7	6.2	3.54 ± 0.16	0.72 ± 0.01
1e	21.6 ± 0.1	4.2	1.6	12.5 ± 0.3	13.6 ± 0.1
1f	2.48 ± 0.04	4.3	2.2	2.46 ± 0.01	2.10 ± 0.03
2a	**95.0 ± 1.9**	**3.0**	**3.6**	**62.5 ± 2.4**	**81.9 ± 2.2**
2b	38 ± 15	3.2	2.6	31 ± 12	8.3 ± 0.2
2c	4.6 ± 0.2	3.5	2.6	5.7 ± 0.1	4.4 ± 0.4
2d	**37.0 ± 2.8**	**5.3**	**3.3**	**36.0 ± 2.7**	**4.4 ± 1.3**
2e	**33.0 ± 2.2**	**7.0**	**0.9**	**9.5 ± 0.2**	**16.0 ± 1.0**

Table 1b
ITC-derived K values for the binding of **1a-1f** and **2a-2e** to the DDD hairpin (Figure 8b).[e]

	K ($\times 10^5$M $^{-1}$)		K($\times 10^5$M $^{-1}$)
1a	**14.6 ± 2.9**	**2a**	**21.1 ± 2.7**
1b	1.2 ± 0.5	**2b**	2.4 ± 1.2
1c	3.1 ± 0.6	**2c**	0.5 ± 0.1
1d	96.4 ± 4.5	**2d**	**7.5 ± 1.3**
1e	0.3 ± 0.1	**2e**	**20.5 ± 9.5**
1f	48.7 ± 1.3		

[a]Average K_{app} values obtained by the ethidium displacement method ($K_{app} = K_e \times C_e/C_{50}$) [b]Ratio of CT DNA(bp):ligand, as determined from the breakpoint of the curve in a plot of Δ Fluorescence vs. CT DNA:ligand ratio.[5c]T_M values obtained from first derivative analysis (ΔA/ΔT vs. ΔT) of the sigmoidal curves A_{260} vs. T; $\Delta T_M = T_M$(CT DNA + ligand)- T_m(CT DNA); [CT DNA] = 75 μM/bp; [ligand] = 2.5 μM.[27d][netropsin] or [methyl green] = 2.0 μM, [CT DNA] = 0.625 μM/bp, and [ethidium bromide] = 5 μM for **1a-1f**; [netropsin] or [methyl green] = 0.5 μM, [CT DNA] = 1.0 μM/bp, and [ethidium bromide] = 0.5 μM for **2a-2e**. Initial addition of netropsin or MG to the CT DNA•ethidium complex results in a 24.3 ± 3.2% or 30.5 ± 4.5% decrease, respectively, in ethidium fluorescence; the new fluorescence value after addition represents the initial fluorescence reading for titrations with compounds **1a-1f** and **2a-2e**. **Red** likely minor groove binder; **green** likely major groove binder. [e] K values (average of triplicate experiments) obtained from ITC titrations of DDD hairpin (10 μM) with ligand (100 μM in syringe).

of methyl green required to achieve 50% inhibition of DNA cleavage (IC_{50}) by BamH1 was 77 μM, the concentration of netropsin required to achieve the same level of cleavage inhibition was greater than 600 μM.[20] In the same manner, whereas the IC_{50} for the putative major groove binder **2d** was 5.4 μM, the IC_{50} for the putative minor groove binder **2a** was 67 μM. Thus, an approximately order of magnitude difference or greater in IC_{50} values was observed for major vs. minor groove binders in plasmid cleavage by BamH1 (Figure 7).

Finally, we examined the sequence selectivity of our synthetic crystal violet derivatives by performing fluorescent intercalator displacement (FID) experiments with a series of oligonucleotides.[21] Three separate hexadecamers, A_5T_5 (5′-GGGAAAAATTTTCCCCC-3′), $(AT)_5$ (5′-GGGA-TATA-TATATCCC-3′) ((AT)5) and G_5C_5 (5′-AAAGGGGG-CCCCCTTT-3′) (all at 10 μM/bp) were titrated with compounds **1a-1f** in the presence of ethidium bromide (5 μM). The percent ethidium displacement at 2 μM of each ligand was recorded (see Supporting Information file), as well as the C_{50} value (Table 2a). As can be seen from the data shown, monomeric CV derivatives showed little sequence discrimination, with only the sterically bulky compound **1b** showing a slight (>3-fold) preference for AT-rich DNA (C_{50}=~2.4 μM for A_5T_5 and $(AT)_5$) over GC rich DNA (C_{50} = 7.2 μM for G5C5).

For the dimeric compounds (Figure 8a and Table 2b), FID assays were used to assess the sequence selectivity of **2a-2e** for hairpin oligonucleotides (Figure 8b) containing consensus sequences for the cancer-relevant transcription factors NFAT1 (5-GAAAAA-3′),[22] STAT6 (5′-TCCTAG-3′),[23] cMyc (5′-CACGTG-3′),[24] as well as the Drew-Dickerson sequence (5′-GAATTC-3′),[25] 5′-ATATAT-3′, and 5′-GGGGGG-3′. Once again, low sequence discrimination was observed, with major-groove binding compound **2d** showing a slight (1.4-fold) preference for binding the AT-rich Drew-Dickerson sequence over the other oligonucleotoides, and minor groove binding compound **2e** showing a modest preference for binding GC-rich sequences over AT-rich sequences. ITC titrations of **1a**, **2a**, **2d**, and **2e** with the six hairpins (Table 2c) also revealed the moderate ~ 6-fold preference of compound **2d** for the AT-rich sequence of NFAT1 over the other oligonucleotides, as well as the preference of **2e** for the GC rich sequences found in the cMyc and GC hairpins.

2.3. Molecular docking studies

Concerning structural factors that may favor major vs. minor groove

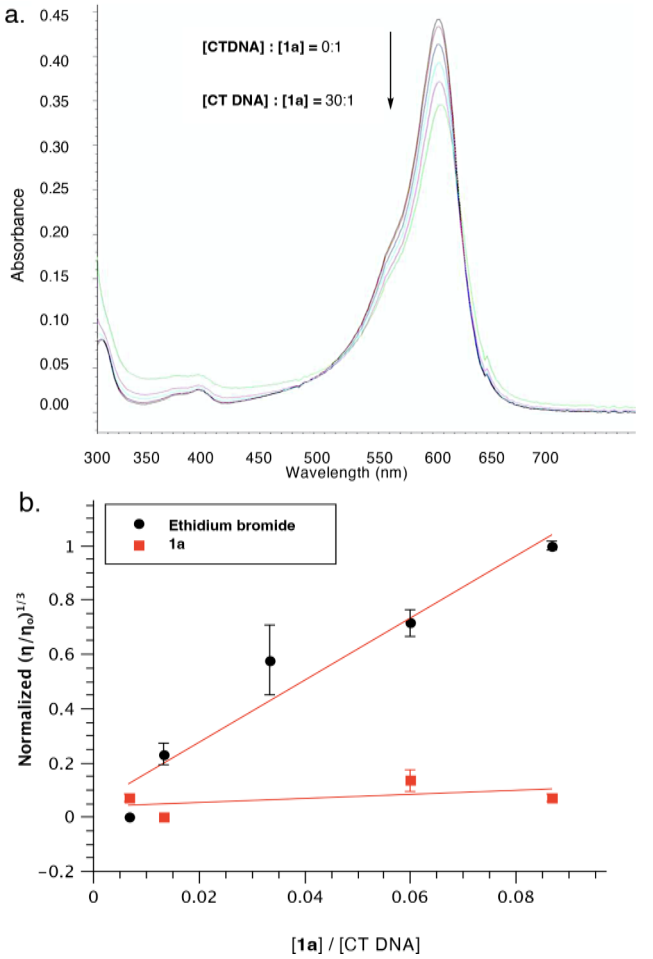

Figure 4. a. UV titration of **1a** in 10 mM Tris-HCl buffer, pH = 7.0: [**1a**] = 5.0 μM; [CT DNA]: [**1a**] = 0:1 (black line); 1:1 (red line); 2:1 (blue line); 5:1 (teal line); 10:1 (purple line); 30:1 (green line). b. Solution viscosity studies for **1a** in 10 mM Tris-HCl, pH = 7.0: [CT DNA] = 300 μM/bp; [ethidium] = 0.0, 2.0, 4.0, 10.0, 18.0, 26.0 μM; [**1a**] = 0.0, 2.0, 4.0, 10.0, 18.0, 26.0 μM. Error bars represent the standard deviation of three replicate experiments. (For interpretation of the references to colour in this figure legend, the reader is referred to the web version of this article.)

binding, ligand docking studies (using AutoDock vina[26]) with the Drew-Dickerson dodecamer (PDB 436D)[25] revealed that whereas compound **1a** localized in the major groove (Figure 9a), compound **1b**, with similar steric bulk, preferred docking in the minor groove. It is noted that the 3,5-dimethyl substitution of **1a** renders a near orthogonal arrangement of the aryl ring planes in this compound, resulting in a ligand span that achieves close electrostatic contact between the electropositive dimethylamino group and the phosphate groups on opposite sides of the major groove. For **2d**, molecular docking with the NFAT sequence (PDB 1OWR)[22] indicates that the *trans* olefin tether is oriented in proximity to the nitrogen and oxygen atoms of the adenine and guanine bases in the major groove (Figure 9b). As can be seen from the electrostatic potential maps of **2d** and the major groove base pairs of 5′-GA-3′ (Figure 9c),[31] the electrophilic character of the dye units is transmitted to the olefin tethers through the connecting π network, possibly allowing a favourable interaction with the *O, N* lone pairs (n → π*)[27] on the edges of the bases in the major groove. For dimer **2e** with the saturated alkoxyalkyl tether, no such interaction with the linker is possible, and the flexible ligand can obtain more favourable hydrophobic interactions in the minor groove. As a result, the high electronegative potential of the major groove[5b,28] appears to favour the binding of ligands that delocalize positive charge from the dye moieties onto the connecting linkers.

3. Conclusions

In summary, we have prepared a series of monomeric and dimeric derivatives of the histochemical stain crystal violet and investigated their DNA binding mode by CD spectroscopy, ITC, viscosity studies, fluorescence spectroscopy, and agarose gel electrophoresis. In the monomeric series, the derivative that displays the strongest preference for major groove occupancy is compound **1a**, possessing the sterically bulky 3,5-dimethylaniline group; the perpendicular arrangement of the aryl rings enforced by this substitution allows the ligand to neatly span the major groove with likely one ionic contact with the phosphate backbone. In the dimeric series, compound **2d**, possessing olefin linkers between the *ortho*-substituted aromatic core and the peripheral dye units, displays the strongest preference for major groove occupancy. Comparing the data obtained for the binding of **2d** and **2e** to DNA, the olefin linkers likely favor major groove binding through charge delocalization from the positively charged dyes to the central region of the molecule, allowing stereoelectronic interactions between the alkene π*orbitals and the N, O lone pair (n) orbitals of the G and A bases. This study highlights the fact that a subtle balance between steric, hydrophobic, and stereoelectronic interactions determines the DNA groove localization of crystal violet derivatives.

Given the generally higher affinities of the dimeric series derivatives, future ligand optimization will be focused on designing dyes that have a combination of steric bulk at the dye termini (in the form of 3,5-dimethylaniline-type substitution), and linker functionality that allow favorable stereoelectronic interactions with the edges of the bases on the floor of the major groove. For the long-term goal of designing sequence specific DNA-binding small molecules capable of interfering with protein binding and gene expression *in vitro* and *in vivo*, future CV derivatives will need to incorporate additional functionality capable of distinguishing sequence context at their major groove binding sites. Alternatively, since it is known that major groove width varies as a function of the DNA sequence,[5] it may be possible to utilize appropriately designed sterically bulky CV derivatives as shape-selective DNA binding molecules.

4. Experimental part

4.1. General

Distilled water was used in all of the experiments. Reagents and solvents were used as supplied, with the following exceptions: CH_2Cl_2 was distilled from CaH_2; Et_2O was distilled from $LiAlH_4$; THF was distilled from sodium benzophenone ketyl; toluene and benzene were dried over 4 Å molecular sieves. Organic extracts were dried over Na_2SO_4, filtered, and concentrated using a rotary evaporator at aspirator pressure (20–30 mmHg). Chromatography refers to flash chromatography and was carried out on SiO_2 (silica gel 60, 230–400 mesh). ^1H and ^{13}C NMR spectra were measured in $CDCl_3$ at 400 MHz and 100 MHz, respectively, using Me_4Si as internal standard. Chemical shifts are reported in parts per million (ppm) downfield (δ) from Me_4Si. For ^1H NMR, multiplicity (s = singlet, d = doublet, dd = doublet of doublets, t = triplet, q = quartet, br = broad, m = multiplet) and coupling constants (in Hz) were reported whenever possible. ^{13}C spectra were recorded with complete proton decoupling.

4.1.1. Synthesis of *1a*

Following a known procedure,[11] 3,5-dimethyl-N,*N*-dimethyl-aniline (1 g, 6.7 mmol) was combined with Mischler's ketone (1.87 g, 7 mmol) in $POCl_3$ (1.1 g, 7 mmol) and the mixture was heated in a sealed tube at 100 °C for 8 h. Upon cooling to room temperature, the mixture was treated with a saturated aqueous solution of K_2CO_3 (20 mL) and ethyl acetate (20 mL), and the phases were separated. The aqueous phase was extracted with ethyl acetate (2 × 20 mL) and the combined organic phases were dried over anhydrous Na_2SO_4, filtered and concentrated *in*

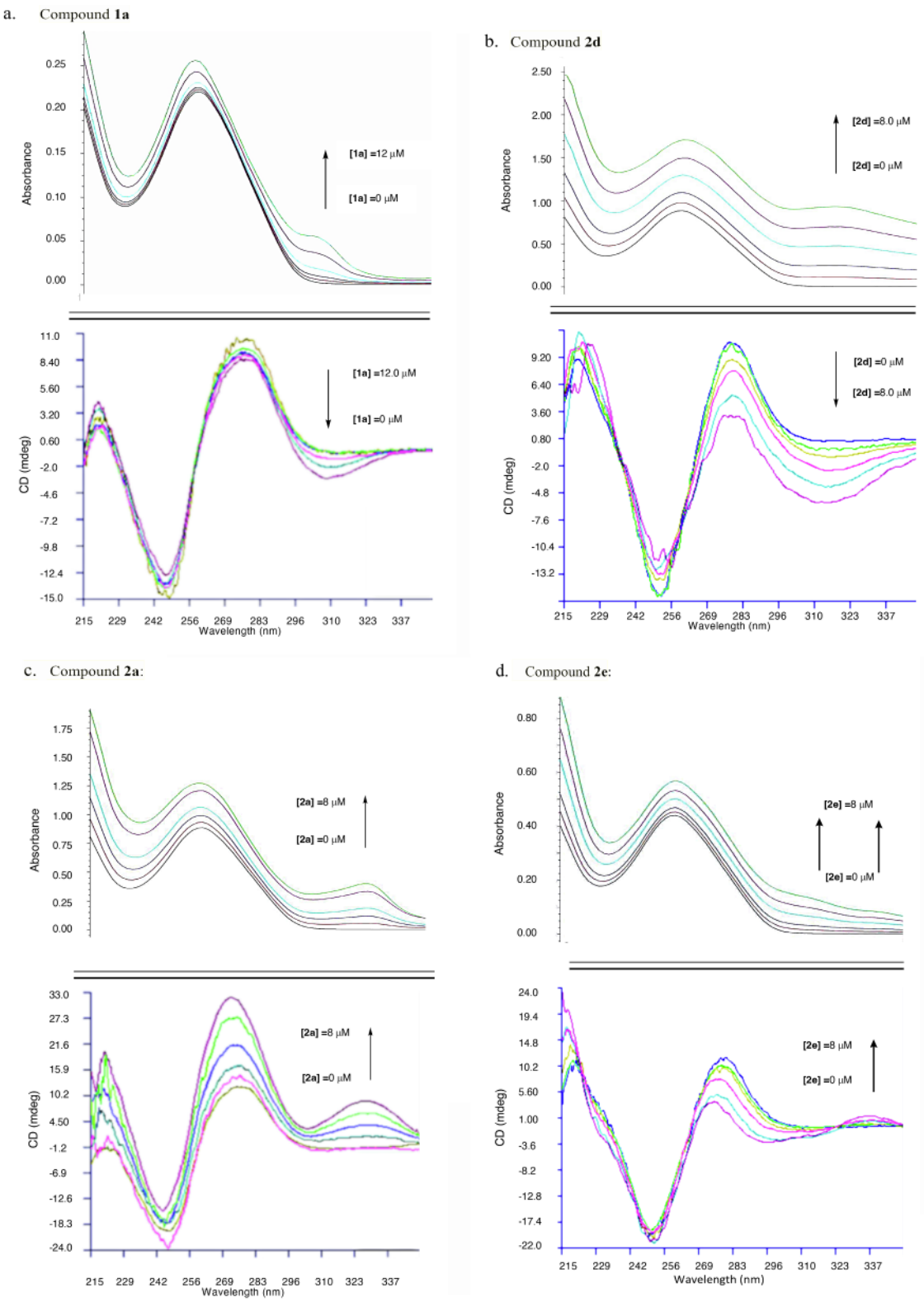

Figure 5. a. The 220–350 nm region of the UV and CD spectra of solutions of DDD hairpin (8.8 μM, 10 mM Tris-HCl, pH = 5.0) in the presence of various concentrations of a. **1a**: 0.0 μM, 0.9 μM, 2.0 μM, 4.0 μM, 8.0 μ, and 12.0 μM; b. **2d**: 0.0 μM, 0.9 μM, 2.0 μM, 4.0 μM, 6.0 μM, and 8.0 μM; c. **2a**: 0.0 μM, 0.9 μM, 2.0 μM, 4.0 μM, 6.0 μM, and 8.0 μM; d. **2e**: 0.0 μM, 0.9 μM, 2.0 μM, 4.0 μM,6.0 μM, and 8.0 μM.

vacuo. The crude material was taken up in EtOAc (20 mL) and extracted with 1 M HCl (3x 20 mL), and the layers were separated. The aqueous phase was further extracted with ethyl acetate (2 × 20 mL) and the combined organic phases were dried over anhydrous Na_2SO_4, filtered and concentrated *in vacuo*. Purification of the residue by size-exclusion chromatography (Sephadex LH-20, chloroform) afforded **1a** (2.2 g, 5.0 mmol, 75%) as a dark blue solid, m.p. 223–226 °C (dec.). **^{1}H NMR** (400 MHz, $CDCl_3$) δ 7.31 (m, 4H, Ar-$H_{metaNMe2}$); 7.25 (m, 2H, Ar-

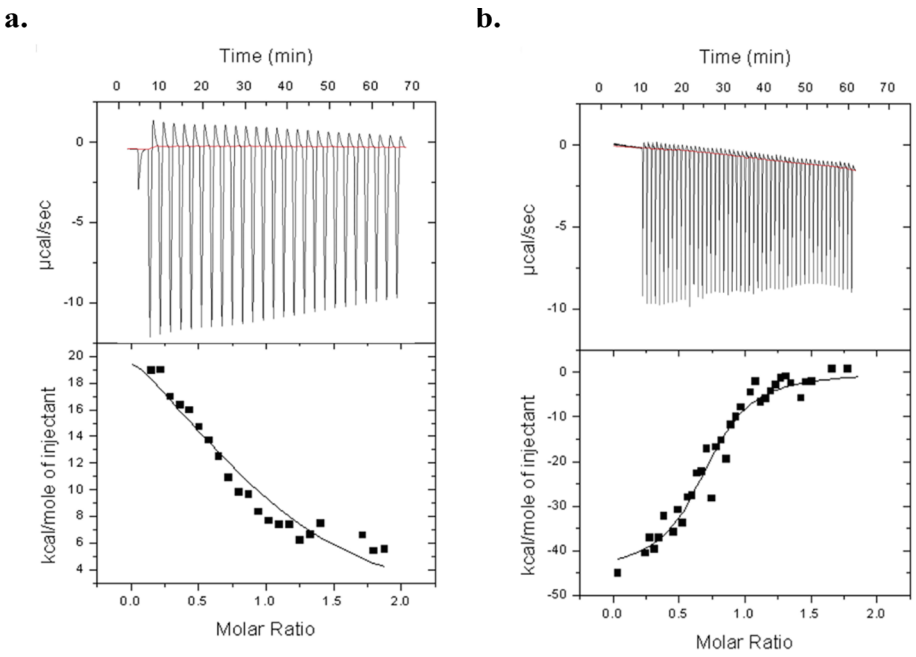

Figure 6. ITC thermograms for the binding of **1a** (a) and **2e** (b) to CT DNA (100 µM/bp, 10 mM Tris-HCl, pH = 7.0). **1a**: $N = 1.0$, $K = 1.9 \pm 0.5x10^5 M^{-1}$, $\Delta H = 29.8 \pm 2.5$ kcal/mol, $\Delta S = 122$ cal/mol•K; **2e**: $N = 0.73$, $K = 2.1 \pm 0.5x10^6 M^{-1}$, $\Delta H = -44.7 \pm 2.2$ kcal/mol, $\Delta S = -120$ cal/mol•K.

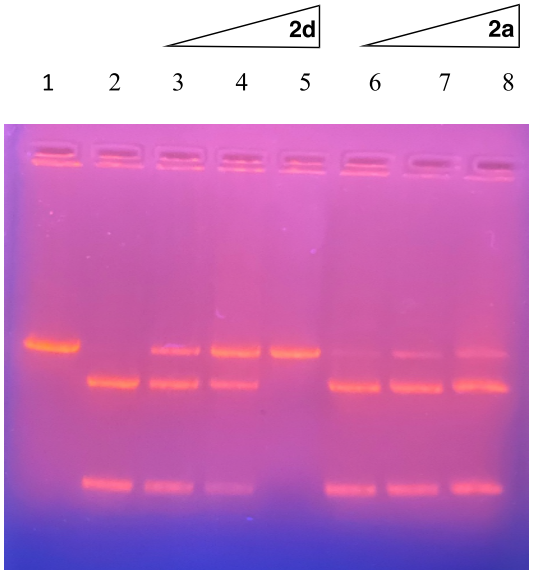

Figure 7. Cleavage of plasmid pUC-19 (linearized with AlwN1, lane 1) by Bam H1 in the presence of **2d** (lanes 3–5) or **2a** (lanes 6–8). Ligand concentrations: lane 2: 0 µM; lane 3: 3 µM **2d**; lane 4: 6 µM **2d**; lane 5: 25 µM **2d**; lane 6: 3 µM **2a**; lane 7: 6 µM **2a**; lane 8: 25 µM **2a**. IC_{50} (**2d**) = 5.4 µM; IC_{50} (**2a**) = 67 µM.

$H_{orthoNMe2}$); 6.98 (m, 4H, Ar-*$H_{orthoNMe2}$*); 3.32 (s, 12H, Ar-N(CH_3)$_2$); 3.21 (s, 6H, Ar-N(CH_3)$_2$); 1.87 (s, 6H, Ar-CH_3). **^{13}C NMR** (100 MHz, $CDCl_3$) δ 156.8 (C = NMe_2), 140.5 (C-Ar_3), 139.1 (C-CH_3), 127.4 (*$C_{meta,paraCNMe2}$*), 114.2 (*$C_{orthoCNMe2}$*), 41.2 (Ar-N(*C*H_3)$_2$), 21.0 (Ar-*C*H_3). **HRMS-ESI** (*m/z*): calculated for $C_{27}H_{34}N_3$ 400.2747 (M^+), found 400.2741 (M^+). **UV** (10 mM Tris-HCl, 0.1 M NaCl, pH = 7.06): λ_{max} 208 nm (ε29758), 256 (8197), 306 (16925), 396 (9300), 614 (118847).

4.1.2. Synthesis of *1b*

3-methyl-4-bromo-*N,N*-dimethylaniline (1 g, 4.69 mmol) was dissolved in THF (10 mL) and cooled to 78 °C. *n*-BuLi (2.1 mL, 2.3 M in cyclohexane, 4.8 mmol) was added dropwise and the solution was stirred at 78 °C for 15 min. Then ethyl-2-methyl-4-dimethylaminobenzoate (345 mg, 1.66 mmol) dissolved in THF (2 mL) was added dropwise at 78 °C. The solution was allowed to warm to room temperature and stir overnight. A solution of 1 M HCl (10 mL) was then added and the mixture was stirred for 30 min. Ethyl acetate (20 mL) was added and the phases were separated. The aqueous phase was further extracted with ethyl acetate (3x 10 mL); the combined organic extracts were once washed with 20 mL sat. aq. NaCl, dried over anhydrous Na_2SO_4, filtered, and concentrated under reduced pressure. Purification of the residue by size-exclusion chromatography (Sephadex LH-20, Chloroform) afforded **1b** (521 mg, 1.12 mmol, 70%) as a blue oil. **^{1}H NMR** (400 MHz, $CDCl_3$) δ 6.95 (d, $J = 9.6$ Hz, 3H, Ar-*$H_{metaNMe2}$*); 6.65 (m, 6H, Ar-*$H_{orthoNMe2}$*); 3.26, (s, 18H, Ar-N(CH_3)$_2$); 1.89 (2, 9H, Ar-CH_3). **^{13}C NMR** (100 MHz, $CDCl_3$) δ 155.1 (*C*-NMe2), 140.1 (*$C_{paraCNMe2}$*), 131.2 (*C*-CH_3, *C*-Ar_3), 115.7 (*$C_{orthoCNMe2}$*), 110.4 (*$C_{orthoCNMe2}$*), 40.5 (Ar-N(*C*H_3)$_2$), 22.2 (Ar-*C*H_3). **HRMS-ESI** (*m/z*): calculated for $C_{28}H_{36}N_3$: 414.2904 (M^+), found 414.2895 (M^+). **UV** (10 mM Tris-HCl, 0.1 M NaCl, pH = 7.06): λ_{max} 210 nm (ε 70957), 256 (34425), 308 (32063), 372 (14442), 618 (122188).

4.1.3. Synthesis of *1c*

4-bromo-*N,N*-dimethylaniline (1 g, 5 mmol) was dissolved in THF (10 mL) and cooled to 78 °C. *n*-BuLi (2.17 mL, 2.3 M in cyclohexane, 5 mmol) was added dropwise and the solution was stirred at 78 °C for 15 min. Then ethyl-6-dimethylamino-2-napthalenecarboxylate (404 mg, 1.66 mmol) dissolved in THF (2 mL) was added dropwise at 78 °C. The solution was allowed to warm to room temperature and stir overnight. A solution of 1 M HCl (10 mL) was then added and the mixture was stirred for 30 min. Ethyl acetate (20 mL) was added and the phases were separated. The aqueous phase was further extracted with ethyl acetate (3x 10 mL); the combined organic extracts were once washed with 20 mL sat. aq. NaCl, dried over anhydrous Na_2SO_4, filtered, and concentrated under reduced pressure. Purification of the residue by size-exclusion chromatography (Sephadex LH-20) afforded **1c** (343 mg, 0.95 mmol, 57%) as a dark green solid, m.p. 197–200 °C (dec). **^{1}H NMR** (400 MHz, $CDCl_3$): δ 7.65 (d, $J = 8.7$ Hz, 1H, Ar-*H*); 7.60 (m, 2H, Ar-*H*); 7.38 (d, $J = 8.8$ Hz, 4H, Ar-*H*); 7.19–7.16 (dd, $J = 2.5, 9.2$ Hz, 2H, Ar-*H*); 6.91 (d, $J = 9.3$ Hz, 5H, Ar-*H*); 3.32 (s, 12H, Ar-N(CH_3)$_2$); 3.18 (s, 6H, Ar-N(CH_3)$_2$). **^{13}C NMR** (100 MHz, $CDCl_3$): δ 178.8 (*C*-Ar_3), 156.2 (*C* =

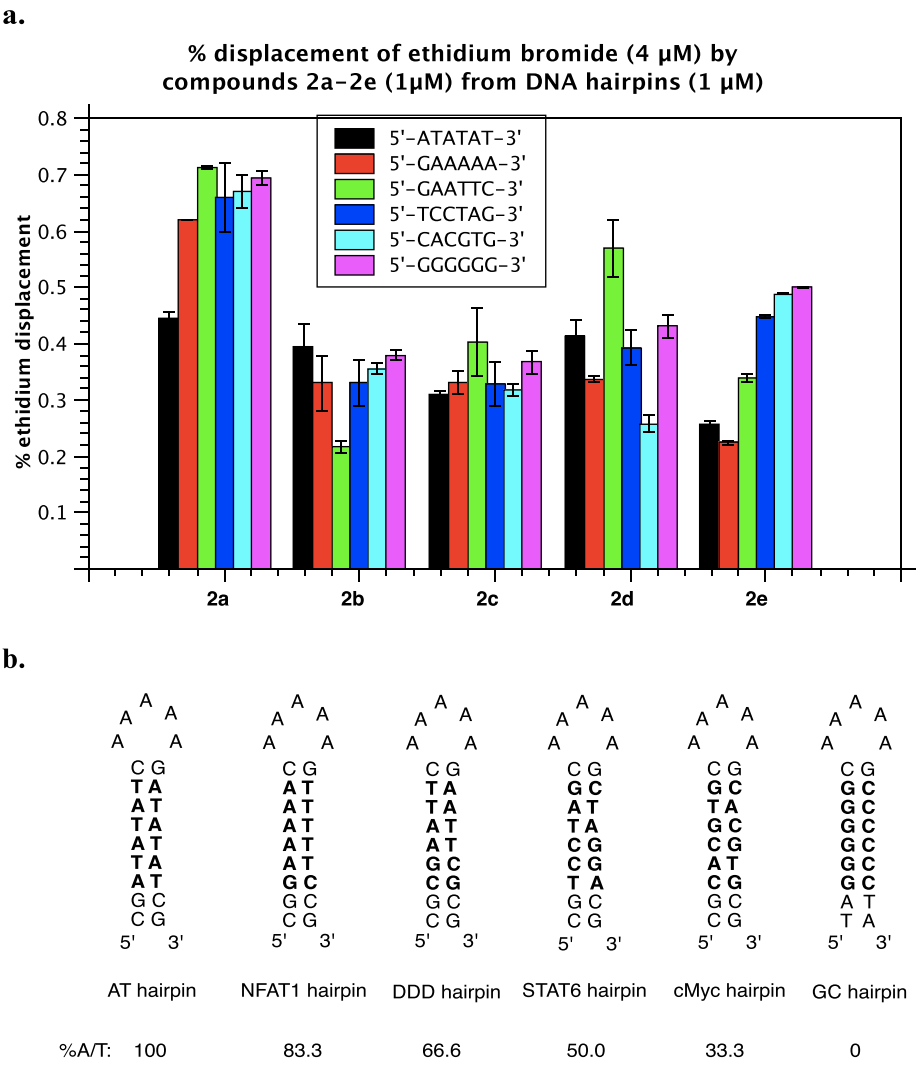

Figure 8. A. chart showing the percent displacement of ethidium bromide (4 μM) from hairpin oligonucleotides 5′-ATATAT-3′, 5′-GAAAAA-3′, 5′-TCCTAG-3′, 5′-CACGTG-3′, 5′-GAATTC-3′, and 5′-GGGGGG-3′ (all at 1 μM) by **2a-2e** (1 μM). b. Structure of hairpin oligonucleotides employed. Experiments performed in 10 mM Tris-HCl buffer, pH = 7.0.

NMe_2),

151.5 ($CNMe_2$), 140.6 (C_{Ar}), 139.2(C_{Ar}), 138. 5 (C_{Ar}), 132.2(C_{Ar}), 131.7 (C_{Ar}), 127.3 (C_{Ar}), 126.2(C_{Ar}), 125.3 (C_{Ar}), 116.6($C_{ortho}CNMe_2$), 113.1($C_{ortho}CNMe_2$), 104.8($C_{ortho}CNMe_2$), 40.9(Ar-N(CH_3)$_2$),

40.4(Ar-N(CH_3)$_2$), **HRMS-ESI** (*m/z*): calculated for $C_{29}H_{32}N_3$ 422.2591 (M^+), found 422.2559 (M^+). **UV** (10 mM Tris-HCl, 0.1 M NaCl, pH = 7.06): λ_{max} 256 nm (ε 42045), 306 (37445), 614 (42815).

4.1.4. Synthesis of *1d*

4-bromo-*N,N*-dimethylaniline (1 g, 5 mmol) was dissolved in THF (10 mL) and cooled to 78 °C. *n*-BuLi (2.17 mL, 2.3 M in cyclohexane, 5 mmol) was added dropwise and the solution was stirred at 78 °C for 15 min. Then ethyl-3-phenyl-4-dimethylaminobenzoate (447 mg, 1.66 mmol) dissolved in THF (2 mL) was added dropwise at 78 °C. The solution was allowed to warm to room temperature and stir for four hours. A solution of 1 M HCl (10 mL) was then added and the mixture was stirred for 30 min. Chloroform (20 mL) was added and the phases were separated. The aqueous phase was further extracted with chloroform (3x 10 mL); the combined organic extracts were once washed with 20 mL sat. aq. NaCl, dried over anhydrous Na_2SO_4, filtered, and concentrated under reduced pressure. Purification of the residue by size exclusion chromatography (Sephadex LH-20) afforded **1d** (420 mg, 0.87 mmol, 52%) as a dark blue solid, m.p. 153–155 °C. **^{1}H NMR** (400 MHz, $CDCl_3$) δ 7.38–7.36 (m, 7H, Ar-*H*); 7.32 (dd, *J* = 6.4, 8.7 Hz, 2H, Ar-*H*); 7.28 (s, 1H, Ar-*H*); 7.18 (s, 1H, Ar-$H_{orthoPh}$); 7.11 (d, *J* = 8.8 Hz, 1H, Ar-$H_{orthoNMe2}$); 6.91 (d, *J* = 9.3 Hz, 4H, Ar-$H_{orthoNMe2}$); 3.31 (s, 12H, Ar-N(CH_3)$_2$); 2.87 (s, 6H, Ar-N(CH_3)$_2$). **^{13}C NMR** (100 MHz, $CDCl_3$) δ 177.7 (*C*-Ar$_3$), 156.6 (*C* = NMe_2), 155.9 (*C*-NMe_2), 141.8 (C_{Ar}), 140.8 (C_{Ar}), 140.1 (C_{Ar}), 137.6 (C_{Ar}), 130.5 (C_{Ar}), 129.2 (C_{Ar}), 128.8 (C_{Ar}), 128.1 (C_{Ar}), 127.3 (C_{Ar}), 126.9 (C_{Ar}), 116.8 ($C_{ortho}CNMe_2$), 112.7 ($C_{ortho}CNMe_2$), 43.2 (Ar-N(CH_3)$_2$), 40.8 (Ar-N(CH_3)$_2$). **HRMS-ESI** (*m/z*): calculated for $C_{31}H_{34}N_3$ 448.2747 (M^+), found 448.2771 (M^+). **UV** (10 mM Tris-HCl, 0.1 M NaCl, pH = 7.06): λ_{max} 210 nm (ε 46240), 308 (17193), 600 (85290).

4.1.5. Synthesis of *1e*

2-phenyl-4-bromo-*N,N*-dimethylaniline (1 g, 3.63 mmol) was dissolved in THF (10 mL) and cooled to 78 °C. *n*-BuLi (1.65 mL, 2.3 M in cyclohexane, 3.8 mmol) was added dropwise and the solution was stirred at 78 °C for 15 min. Then ethyl-4-dimethylaminobenzoate (233 mg, 1.21 mmol) dissolved in THF (2 mL) was added dropwise at 78 °C. The solution was allowed to warm to room temperature and stir for 4 h. A solution of 1 M HCl (10 mL) was then added and the mixture was stirred for 30 min. Chloroform (20 mL) was added and the phases were separated. The aqueous phase was further extracted with chloroform (3x 10 mL); the combined organic extracts were once washed with 20 mL

Table 2
A. C_{50} data for the binding of **1a-1f** to A_5T_5, $(AT)_5$, and G_5C_5. b. C_{50} data for the binding of **2a-2e** to hairpin oligonucleotides $(AT)_3$, NFAT1, STAT6, cMyc, Drew-Dickerson, and G_6. c. ITC-derived *K* values (average of triplicate experiments) for the binding of **1a**, **2a**, **2d**, and **2e** (100 μM in syringe) to DNA hairpins oligonucleotides (10 μM).

a.

	A_5T_5 (μM)	**$(AT)_5$** (μM)	**G_5C_5** (μM)
1a	1.86 ± 0.01	1.57 ± 0.05	2.05 ± 0.11
1b	2.40 ± 0.02	2.30 ± 0.03	7.21 ± 0.63
1c	0.52 ± 0.01	0.32 ± 0.02	0.88 ± 0.01
1d	2.61 ± 0.02	2.75 ± 0.21	2.99 ± 0.01
1e	1.83 ± 0.01	1.81 ± 0.01	2.09 ± 0.06
1f	3.13 ± 0.01	2.71 ± 0.03	3.36 ± 0.07

b.

	$(AT)_3$ (μM)	**NFAT1** (μM)	**DDD** (μM)	**STAT6** (μM)	**cMyc** (μM)	**G_6** (μM)
2a	1.11 ± 0.03	0.69 ± 0.03	0.54 ± 0.02	0.56 ± 0.01	0.57 ± 0.03	0.51 ± 0.11
2b	1.36+0.04	1.23 ± 0.08	1.47 ± 0.03	1.32 ± 0.20	1.42 ± 0.05	1.25 ± 0.16
2c	1.52 ± 0.02	2.22 ± 0.13	1.27 ± 0.34	1.91 ± 0.25	1.95 ± 0.15	1.32 ± 0.12
2d	1.21 ± 0.07	1.27 ± 0.05	0.78 ± 0.08	1.12 ± 0.04	1.80 ± 0.06	1.10 ± 0.04
2e	2.08 ± 0.01	2.64 ± 0.05	1.57 ± 0.02	1.09 ± 0.02	1.56 ± 0.01	1.00 ± 0.03

c.

	$(AT)_3$ *K* ($x10^5 M^{-1}$)	**NFAT1** *K* ($x10^5 M^{-1}$)	**DDD** *K* ($x10^5 M^{-1}$)	**STAT6** *K* ($x10^5 M^{-1}$)	**cMyc** *K* ($x10^5 M^{-1}$)	**G_6** *K* ($x10^5 M^{-1}$)
1a	0.21 ± 0.07	0.19 ± 0.04	14.6 ± 2.9	1.06 ± 0.63	12.6 ± 3.4	28.3 ± 6.7
2a	0.32 ± 0.08	1.14 ± 0.32	21.1 ± 2.7	1.80 ± 0.66	1.14 ± 0.29	52.8 ± 22.7
2d	5.79 ± 4.29	49.8 ± 10.3	7.54 ± 1.26	2.22 ± 0.42	0.32 ± 0.15	0.18 ± 0.09
2e	1.3 ± 0.38	29.1 ± 9.2	20.5 ± 9.6	1.32 ± 0.57	50.6 ± 7.65	36.5 ± 14.4

sat. aq. NaCl, dried over anhydrous Na_2SO_4, filtered, and concentrated under reduced pressure. Purification of the residue by size exclusion chromatography (Sephadex LH-20) afforded **1e** (264 mg, 0.47 mmol, 39%) as a dark blue solid, m.p. 116–118 °C (dec). **^{1}H NMR** (400 MHz, $CDCl_3$) δ 7.41–7.34 (m, 14H, Ar-*H*); 7.26–7.25 (d, J = 2.2 Hz, 2H, Ar-$H_{orthoPh}$); 7.17 (d, J = 8.9 Hz, 2H, Ar-$H_{orthoNMe2}$); 6.99 (d, J = 9.2 Hz, 2H, Ar-$H_{orthoNMe2}$); 3.37 (s, 6H, Ar-N(CH_3)$_2$); 2.92 (s, 12H, Ar-N(CH_3)$_2$). **^{13}C NMR** (100 MHz, $CDCl_3$) δ 177.2 (*C*-Ar_3), 156.9 (*C*-NMe_2), 156.4 (*C* = NMe_2), 142.2 (C_{Ar}), 140.9 (C_{Ar}), 140.5 (C_{Ar}), 138.0 (C_{Ar}), 130.5 (C_{Ar}), 129.2 (C_{Ar}), 128.8 (C_{Ar}), 128.2 (C_{Ar}), 127.4 (C_{Ar}), 127.1 (C_{Ar}), 116.9 (C_{ortho}CNMe2), 113.2 (C_{ortho}CNMe2), 43.3 (ArN(CH_3)$_2$), 40.9 (Ar-N(CH_3)$_2$). **HRMS-ESI** (*m/z*): calculated for $C_{37}H_{38}N_3$ 524.3060 (M^+), found 524.3068 (M^+). **UV** (10 mM Tris-HCl, 0.1 M NaCl, pH = 7.06): λ_{max} 232 nm (ε 715875), 582 (76617).

4.1.6. Synthesis of *1f*

2-phenyl-4-bromo-*N,N*-dimethylaniline (1 g, 3.63 mmol) was dissolved in THF (10 mL) and cooled to 78 °C. *n*-BuLi (1.65 mL, 2.3 M in cyclohexane, 3.8 mmol) was added dropwise and the solution was stirred at 78 °C for 15 min. Then ethyl-3-phenyl-4-dimethylaminobenzoate (325 mg, 1.21 mmol) dissolved in THF (2 mL) was added dropwise at 78 °C. The solution was allowed to warm to room temperature and stir for 4 h. A solution of 1 M HCl (10 mL) was then added and the mixture was stirred for 30 min. Chloroform (20 mL) was added and the phases were separated. The aqueous phase was further extracted with chloroform (3x 10 mL); the combined organic extracts were once washed with 20 mL sat. aq. NaCl, dried over anhydrous Na_2SO_4, filtered, and concentrated under reduced pressure. Purification of the residue by size exclusion chromatography (Sephadex LH-20, chloroform) afforded **1f** (503 mg, 0.78 mmol, 65%) as a blue solid, m.p. 80–83 °C (dec). **^{1}H NMR** (400 MHz, $CDCl_3$) δ 7. 51 (d, J = 7.3 Hz, 3H, Ar-*H*); 7.45–7.38 (m, 15H, Ar-*H*); 7.32 (d, J = 2.3 Hz, 3H, Ar-$H_{orthoPh}$); 7.24 (d, J = 9.0 Hz, 3H, Ar-$H_{orthoNMe2}$); 2.96 (s, 18H, Ar-N(CH_3)$_2$). **^{13}C NMR** (100 MHz, $CDCl_3$) δ 176.8 (*C*-Ar_3), 157.3 (*C*-NMe_2)), 142.8 (C_{Ar}), 140.9 (C_{Ar}), 138.6 (C_{Ar}), 130.5 (C_{Ar}), 129.0 (C_{Ar}), 128.9 (C_{Ar}), 128.2 (C_{Ar}), 127.5 (C_{Ar}), 117.3 (C_{ortho}CNMe2), 43.5 (Ar-N(CH_3)$_2$). **HRMS-ESI** (*m/z*): calculated for $C_{43}H_{42}N_3$ 600.3373 (M^+), found 600.3376 (M^+). **UV** (10 mM Tris-HCl, 0.1 M NaCl, pH = 7.06): λ_{max} 260 nm (ε 136050), 320 (53177), 602 (42885).

4.1.7. Synthesis of *2a*

1,2-diiodobenzene (330 mg, 1 mmol) and 2-(methoxycarbonyl)-phenylboronic acid (396 mg, 2.2 mmol) were dissolved in a 4:1 toluene: water mixture (10 mL) and K_2CO_3 (607 mg, 4.4 mmol) and $Pd(PPh_3)_4$ (116 mg, 0.1 mmol, 10 mol%) were added. The mixture was heated to 95 °C under argon and stirred for 24 h. After cooling to room temperature, water (10 mL) and ether (10 mL) were added, and the phases were separated. The aqueous phase was extracted twice with ether (2x10 mL) and the combined organic phases were dried over anhydrous sodium sulfate, filtered, and concentrated *in vacuo*. The crude oil was taken up in 2:1 hexanes:ethyl acetate and rapidly flushed through a plug of silica gel; concentration *in vacuo* furnished material sufficiently pure for the next step. 4-bromo-*N,N*-dimethylaniline (1 g, 5 mmol) was dissolved in THF (10 mL) and cooled to 78 °C. *n*-BuLi (2.17 mL, 2.3 M in cyclohexane, 5 mmol) was added dropwise and the solution was stirred at 78 °C for 15 min. Then the diester intermediate from the previous step (~1 mmol) dissolved in THF (2 mL) was added dropwise at 78 °C. The solution was allowed to warm to room temperature and stir for four hours. A solution of 1 M HCl (10 mL) was then added, and the mixture was stirred for 30 min. Chloroform (20 mL) was added, and the phases were separated. The aqueous phase was further extracted with chloroform (3 × 10 mL); the combined organic extracts were once washed with 20 mL sat. aq. NaCl, dried over anhydrous Na_2SO_4, filtered, and concentrated under reduced pressure. Purification by size exclusion chromatography (Sephadex LH-20, Chloroform) afforded **2a** (340 mg, 0.43 mmol, 43%) as a dark green solid, m.p. 220–221 °C. **^{1}H NMR** (400 MHz, $CDCl_3$) δ 7.40 (t, J = 8.1 Hz, 2H, Ar-*H*); 7.28 (m, 4H, Ar-*H*); 7.10 (d, J = 7.5 Hz, 2H, Ar-*H*); 7.01 (d, J = 7.4 Hz, 2H, Ar-*H*); 6.88 (m, 7H, Ar-*H*); 6.77–6.71 (m, 7H, Ar-*H*); 6.57 (d, J = 9.1 Hz, 4H, Ar-$H_{orthoNMe2}$); 3.46 (s, 10*H*, Ar-N(CH_3)$_2$); 3.21 (s, 14H, Ar-N(CH_3)$_2$). **^{13}C NMR** (100 MHz, $CDCl_3$) δ 175.8 (*C*-Ar_3), 156.9 (*C* = NMe_2), 155.7 (*C*-NMe_2), 144.7 (C_{Ar}), 141.2 (C_{Ar}), 138.8 (C_{Ar}), 138.7 (C_{Ar}), 137.8 (C_{Ar}), 135.2 (C_{Ar}), 132.6

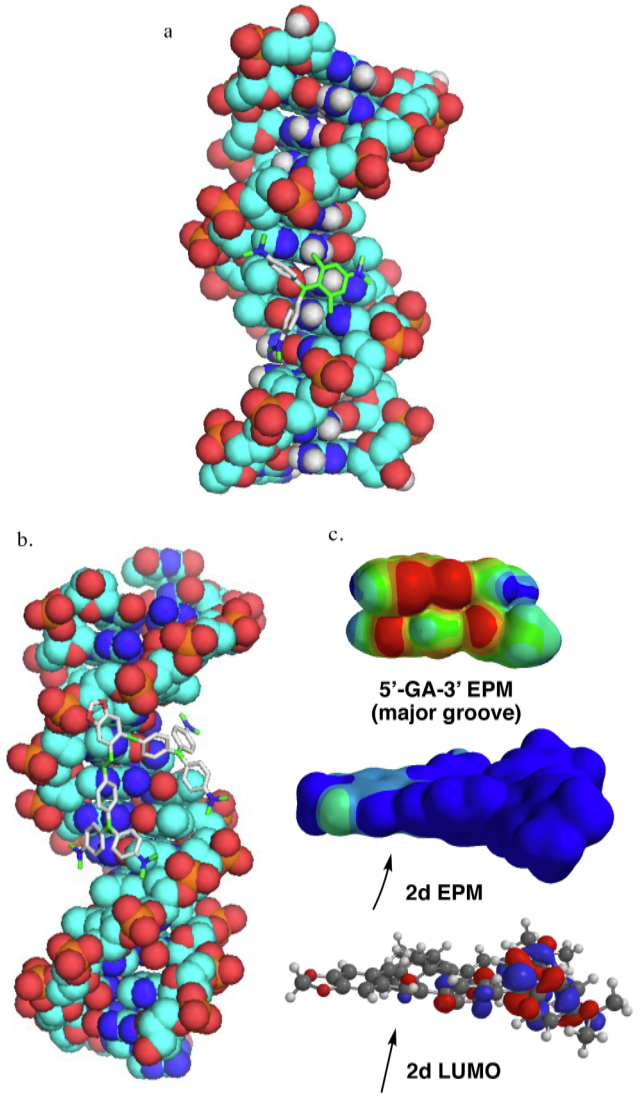

Figure 9. A. model for the binding of ligand **1a** in the major groove of Drew Dickerson dodecamer DNA (5′-CGCGAATTCGCG-3′). b. Model for the binding of ligand **2d** in the major groove of the NFAT1 sequence (5′-GGAAAAA-3′). c. Electrostatic potential maps for the major groove base pairs of 5′-GA-3′ and **2d**, and LUMO map of **2d**.[31] Arrow points to the alkene moiety.

(C_{Ar}), 132.4 (C_{Ar}), 132.3 (C_{Ar}), 128.1 (C_{Ar}), 127.8 (C_{Ar}), 127.6 (C_{Ar}), 126.8 (C_{Ar}), 114.6 ($C_{orthoCNMe2}$), 112.8 ($C_{orthoCNMe2}$), 41.6 (Ar-N(CH_3)$_2$), 40.9 (Ar-N(CH_3)$_2$). **HRMS-ESI** (*m/z*): calculated for $C_{52}H_{52}N_4$ 366.2091 (M^{2+}), found 366.2094 (M^{2+}). **UV** (10 mM Tris-HCl, 0.1 M NaCl, pH = 7.06): λ_{max} 202 nm (ε 204505), 322 (56710), 438 (62422), 638 (209425).

4.1.8. Synthesis of **2b**

5,6-dibromo-1,3-benzodioxole (280 mg, 1 mmol) and 4-(methoxycarbonyl)phenylboronic acid (540 mg, 3.0 mmol) were dissolved in a 4:1 toluene:water mixture (10 mL) and K_2CO_3 (690 mg, 5.0 mmol) and $Pd(PPh_3)_4$ (174 mg, 0.15 mmol, 15 mol%) were added. The mixture was heated to 95 °C under argon and stirred for 48 h. After cooling to room temperature, water (10 mL) and ether (10 mL) were added, and the phases were separated. The aqueous phase was extracted twice with ether (2x10 mL) and the combined organic phases were dried over anhydrous sodium sulfate, filtered, and concentrated *in vacuo*. The crude oil was taken up in 2:1 hexanes:ethyl acetate and rapidly flushed through a plug of silica gel; concentration *in vacuo* furnished material sufficiently pure for the next step. 4-bromo-*N,N*-dimethylaniline (1 g, 5 mmol) was dissolved in THF (10 mL) and cooled to 78 °C. *n*-BuLi (2.17 mL, 2.3 M in cyclohexane, 5 mmol) was added dropwise and the solution was stirred at 78 °C for 15 min. Then the diester intermediate from the previous step (~1 mmol) dissolved in THF (2 mL) was added dropwise at 78 °C. The solution was allowed to warm to room temperature and stir for four hours. A solution of 1 M HCl (10 mL) was then added, and the mixture was stirred for 30 min. Chloroform (20 mL) was added, and the phases were separated. The aqueous phase was further extracted with chloroform (3x 10 mL); the combined organic extracts were once washed with 20 mL sat. aq. NaCl, dried over anhydrous Na_2SO_4, filtered, and concentrated under reduced pressure. Purification by size exclusion chromatography (Sephadex LH-20, chloroform) afforded **2b** (521 mg, 0.63 mmol, 63%) as a dark green solid, m.p. 117–120 °C (dec). **^{1}H NMR** (400 MHz, $CDCl_3$) δ 7.21 (m, 12H, Ar-*H*); 7.18 (m, 4H, Ar-*H*); 6.93 (s, 2H, Ar-*H*); 6.85 (m, 8H, Ar-$H_{orthoNMe2}$); 6.04 (s, 2H, O-CH_2-O); 3.31 (m, 24H, Ar-N(CH_3)$_2$). **^{13}C NMR** (100 MHz, $CDCl_3$) δ 176.5 (*C*-Ar$_3$), 156.8 (*C*-NMe$_2$), 148.2 (C_{Ar}), 146.3 (C_{Ar}), 140.6 (C_{Ar}), 137.6 (C_{Ar}), 134.7 (C_{Ar}), 133.2 (C_{Ar}), 130.3 (C_{Ar}), 127.0 (C_{Ar}), 113.8 ($C_{orthoCNMe2}$), 110.5 ($C_{orthoCNMe2}$), 101.9 (O-*C*H$_2$-O), 41.2 (Ar-N(*C*H$_3$)$_2$). **HRMS-ESI** (*m/z*): calculated for $C_{53}H_{52}N_4O_2$ 388.2039 (M^{2+}), found 388.2046 (M^{2+}). **UV** (10 mM Tris-HCl, 0.1 M NaCl, pH = 7.06): λ_{max} 210 nm (ε 161235), 308 (71936), 440 (54252), 628 (214303).

4.1.9. Synthesis of **2c**

5,6-diethynyl-1,3-benzodioxole[33] (170 mg, 1 mmol) and methyl-4-iodobenzoate (786 mg, 3 mmol) were dissolved in triethylamine (3 mL) and CuI (4 mg, 0.15 mmol) and $Pd(PPh_3)_4$ (116 mg, 0.1 mmol, 10 mol%) were added. The mixture was heated to 60 °C under argon for 24 h. After cooling to room temperature, water (10 mL) and ether (10 mL) were added, and the phases were separated. The aqueous phase was extracted twice with ether (2x10 mL) and the combined organic phases were dried over anhydrous sodium sulfate, filtered, and concentrated *in vacuo*. The crude material was taken up in 2:1 hexanes:ethyl acetate and rapidly flushed through a plug of silica gel; concentration *in vacuo* furnished material sufficiently pure for the next step. 4-bromo-*N,N*-dimethylaniline (1 g, 5 mmol) was dissolved in THF (10 mL) and cooled to 78 °C. *n*-BuLi (2.17 mL, 2.3 M in cyclohexane, 5 mmol) was added dropwise and the solution was stirred at 78 °C for 15 min. Then the diester intermediate from the previous step (~1 mmol) dissolved in THF (2 mL) was added dropwise at 78 °C. The solution was allowed to warm to room temperature and stir for four hours. A solution of 1 M HCl (10 mL) was then added, and the mixture was stirred for 30 min. Chloroform (20 mL) was added, and the phases were separated. The aqueous phase was further extracted with chloroform (3x 10 mL); the combined organic extracts were once washed with 20 mL sat. aq. NaCl, dried over anhydrous Na_2SO_4, filtered, and concentrated under reduced pressure. Purification by size exclusion chromatography (Sephadex LH-20, Chloroform) afforded **2c** (478 mg, 0.53 mmol, 53%) as a dark green solid, m.p. 110–113 °C. **^{1}H NMR** (400 MHz, $CDCl_3$) δ 7.67 (d, *J* = 7.1 Hz, 4H, Ar-*H*); 7.32 (m, 13H, Ar-*H*); 6.95 (d, *J* = 7.7 Hz, 9H, Ar-$H_{orthoNMe2}$); 6.06 (s, 2H, O-CH_2-O); 3.35 (m, 24H, Ar-N(CH_3)$_2$). **^{13}C NMR** (100 MHz, $CDCl_3$) δ 175.6 (*C*-Ar$_3$), 156.9 (*C*-NMe$_2$), 148.5 (C_{Ar}), 140.6 (C_{Ar}), 139.2 (C_{Ar}), 134.9 (C_{Ar}), 131.4 (C_{Ar}), 128.3 (C_{Ar}), 127.2 (C_{Ar}), 119.9 ($C_{orthoCNMe2}$), 114.1 ($C_{orthoCNMe2}$), 111.7 (C_{sp}), 102.3 (O-*C*H$_2$-O), 92.0 (C_{sp}), 41.3 (Ar-N(*C*H$_3$)$_2$). **HRMS-ESI** (*m/z*): calculated for $C_{57}H_{52}N_4O_2$ 412.2040 (M^{2+}), found 412.2037 (M^{2+}). **UV** (10 mM Tris, 0.1 M NaCl, pH = 7.06): λ_{max} 204 nm (ε 317547), 266 (128225), 322 (121537), 462 (103221), 640 (214303).

4.1.10. Synthesis of **2d**

Methyl 4-[(diethoxyphosphinyl)methyl]benzoate[2] (429 mg, 1.5 mmol) was dissolved in THF (5 mL) and cooled to 0 °C. Then sodium hydride (60 mg, 1.5 mmol, 60% dispersion in mineral oil) was added and the mixture was allowed to stir for 30 min. Then 1,3-benzodioxole-5,6-dicarboxyaldehyde (174.8 mg, 1 mmol) was added and the mixture was stirred overnight. Water (10 mL) and ether (10 mL) were added, and

the phases were separated. The aqueous phase was extracted twice with ether (2x10 mL) and the combined organic phases were dried over anhydrous sodium sulfate, filtered, and concentrated *in vacuo*. The crude material was taken up in 3:1 hexanes:ethyl acetate and rapidly flushed through a plug of silica gel; concentration *in vacuo* furnished material sufficiently pure for the next step. 4-bromo-*N,N*-dimethylaniline (1 g, 5 mmol) was dissolved in THF (10 mL) and cooled to −78 °C. *n*-BuLi (2.17 mL, 2.3 M in cyclohexane, 5 mmol) was added dropwise and the solution was stirred at −78 °C for 15 min. Then the diester intermediate from the previous step (~1 mmol) dissolved in THF (2 mL) was added dropwise at −78 °C. The solution was allowed to warm to room temperature and stir for four hours. A solution of 1 M HCl (10 mL) was then added, and the mixture was stirred for 30 min. Chloroform (20 mL) was added, and the phases were separated. The aqueous phase was further extracted with chloroform (3x 10 mL); the combined organic extracts were once washed with 20 mL sat. aq. NaCl, dried over anhydrous Na_2SO_4, filtered, and concentrated under reduced pressure. Purification by size exclusion chromatography (Sephadex LH-20, Chloroform) afforded **2d** (360 mg, 0.4 mmol, 40%) as a dark green solid, m.p. 191–195 °C (dec). **^{1}H NMR** (400 MHz, $CDCl_3$) δ 7.76 (m, 8H, Ar-*H*); 7.39 (m, 12H, Ar-*H*); 7.15 (s, 2H, Ar-*H*); 7.00 (d, $J = 9.2$ Hz, 8H, Ar-$H_{orthoNMe2}$); 6.05 (s, 2H, O-CH_2-O); 3.37 (s, 24H, Ar-N(CH_3)$_2$). **^{13}C NMR** (100 MHz, $CDCl_3$) δ 176.8 (*C*-Ar$_3$), 156.8 (*C*-NMe_2), 148.6 (C_{Ar}), 142.7 (C_{Ar}), 140.7 (C_{Ar}), 138.4 (C_{Ar}), 135.9 (C_{Ar}), 135.1 (C_{Ar}), 133.3 (C_{sp2}), 133.2 (C_{sp2}), 130.6 (C_{Ar}), 130.5 (C_{Ar}), 130.3(C_{Ar}), 129.5(C_{sp2}), 128.8 (C_{Ar}), 127.2 (C_{Ar}), 126.7 (C_{sp2}), 113.8 ($C_{orthoCNMe2}$), 106.1 (O-CH_2-O), 41.3 (Ar-N(CH_3)$_2$). **HRMS-ESI** (*m/z*): calculated for $C_{57}H_{56}N_4O_2$ 414.2196 (M^{2+}), found 414.2184 (M^{2+}). **UV** (0.1 M Tris, 0.1 M NaCl, pH = 7.06): λ_{max} 204 nm (ε 297848), 314 (110774), 628 (214303).

4.1.11. Synthesis of **2e**

1,2-benzenedimethanol (138 mg, 1 mmol) and methyl-4-hydroxybenzoate (334 mg, 2.2 mmol) were dissolved in THF (5 mL) and triphenylphosphine (577 mg, 2.2 mmol) was added. The solution was stirred at room temperature and diisopropylazodicarboxylate (433 uL, 2.2 mmol) was added dropwise and the solution was stirred for 2 h. Water (10 mL) and ether (10 mL) were added, and the phases were separated. The aqueous phase was extracted twice with ether (2x10 mL) and the combined organic phases were dried over anhydrous sodium sulfate, filtered, and concentrated *in vacuo*. The crude material was chromatographed over silica gel (10:1 → 4:1 hexanes:ethyl acetate) to afford material the intermediate diester. 4-bromo-*N,N*-dimethylaniline (1 g, 5 mmol) was dissolved in THF (10 mL) and cooled to −78 °C. *n*-BuLi (2.17 mL, 2.3 M in cyclohexane, 5 mmol) was added dropwise and the solution was stirred at −78 °C for 15 min. Then the diester intermediate from the previous step (~1 mmol) dissolved in THF (2 mL) was added dropwise at −78 °C. The solution was allowed to warm to room temperature and stir for four hours. A solution of 1 M HCl (10 mL) was then added, and the mixture was stirred for 30 min. Chloroform (20 mL) was added, and the phases were separated. The aqueous phase was further extracted with chloroform (3x 10 mL); the combined organic extracts were once washed with 20 mL sat. aq. NaCl, dried over anhydrous Na_2SO_4, filtered, and concentrated under reduced pressure. Purification by size exclusion chromatography (Sephadex LH-20, chloroform) afforded **2e** (529 mg, 0.61 mmol, 61%) as a dark green solid, m.p. 242–245 °C. **^{1}H NMR** (400 MHz, $CDCl_3$) δ 7.49 (m, 2H, Ar-*H*); 7.35 (m, 3H, Ar-*H*); 7.33–7.29 (m, 12H, Ar-*H*); 7.13 (d, $J = 8.9$ Hz, 4H, Ar-H_{orthoO}); 6.83 (d, $J = 9.3$ Hz, 8H, Ar-$H_{orthoNMe2}$); 5.32 (s, 4H, ArCH_2O); 3.23 (s, 24H, Ar-N(CH_3)$_2$)). **^{13}C NMR** (100 MHz, $CDCl_3$) δ 177.6 (*C*-Ar$_3$), 163.6 (*C*-OCH_2), 156.6 (*C*-NMe_2), 140.6 (C_{Ar}), 137.7 (C_{Ar}), 134.2 (C_{Ar}), 131.9 (C_{Ar}), 129.2 (C_{Ar}), 128.8 (C_{Ar}), 126.8 (C_{Ar}), 115.3 ($C_{orthoCNMe2}$), 113.3 ($C_{orthoCNMe2}$), 68.6 (Ar*C*H$_2$O), 40.9 (Ar-N(*C*H$_3$)$_2$). **HRMS-ESI** (*m/z*): calculated for $C_{54}H_{56}N_4O_2$ 396.2196 (M^{2+}), found 396.2215 (M^{2+}). **UV** (10 mM Tris, 0.1 M NaCl, pH = 7.06): λ_{max} 204 nm (ε 114333), 296 (29027), 448 (62834), 570 (174000).

4.2. Competitive ethidium bromide displacement

Constant concentrations of CT-DNA (1.0 μM/bp) and EtBr (0.5 μM) in the presence or absence of netropsin (0.5 μM) or methyl green (0.5 μM) were titrated with increasing concentrations of the ligands **1a**-**1f** and **2a**-**2e** (from 100 μM and 10 μM stock solutions) in buffer (10 mM Tris-HCl, pH = 7.0). The maximum emission wavelength was 590 nm when the excitation wavelength was 520 nm. Fluorescence titrations were recorded from 520 nm to 692 nm after an equilibration period of 3 min. Ex Slit (nm) = 10.0; Em Slit (nm) = 10.0; Scan Speed (nm/min) = 200. $K_{app} = 9.5x10^6\ M^{-1} \times C_{ethidium}/C_{50}$.

4.3. Thermal denaturation studies

UV thermal denaturation samples (2 mL) were prepared by mixing CT-DNA in 10 mM Tris-HCl buffer (pH 7.0) in 1 cm path length quartz cuvettes. The DNA to ligand ratio was 30:1. Absorbance readings were taken for temperature ranging from 25 °C to 95 °C. Temperature was increased gradually with a speed of 1 °C/min with an absorbance reading every 2 °C. First derivative plots were used to determine the T_M value.

4.4. Solution viscosity studies

Viscosity experiments were performed with an Ostwald viscometer in a constant water bath at 23.0 ± 1 °C. Solutions of constant DNA concentrations (300 μM/bp) and varying ligand concentrations in 10 mM Tris-HCl buffer (pH 7.0) were incubated for 30 min. A digital stopwatch was used to record the flow time. The relative viscosity was calculated as from the following equation:

$\eta = t\text{-}t_0/t_0$.

Where t_o and t are the flow time in the absence and presence of the ligand. η is the viscosity in the presence of the ligand and η_o is the viscosity in the absence of ligand. The data were graphed as $(\eta/\eta_o)^{1/3}$ vs. [ligand]/[DNA].

4.5. Circular dichroism and UV studies

Small aliquots (0.6–5.0 μL) of concentrated ligands **1a**-**1f** and **2a**-**2e** (1 mM) were added to a solution (2 mL, 10 mM tris-HCl, pH 5.0) of CT-DNA (80 μM/bp) or DDD hairpin (8.8 μM), inverted twice, and incubated for 5 min at 20 °C. The CD spectra were then recorded as an average of three scans from 215 to 350 nm and data recorded in 0.5 nm increments. UV spectra were collected under identical conditions over the same wavelength range.

4.6. Isothermal titration calorimetry studies

ITC thermograms were recorded for titrations performed at 30 °C (except for compound **2e** performed at 27 °C with 50 injections, 5 μL each, 180 s duration) under the following conditions: DP = 6, 307 rpm, 10 μL injections, 10 s duration with 120 s, 2 s filter, initial delay of 120 s, total of 25 injections (Microcal VP-ITC). The initial conditions for the titrations involved 100 μM ligand in the syringe and 100 μM/bp CT DNA or 10 μM hairpins in the cell, common buffer 10 mM Tris-HCl, pH = 7.0. Prior to data analysis in Origin software, subtraction of buffer to CT DNA titrations under identical conditions was performed to account for heats of dilution. A single-site binding model was applied to obtain vales of *K*, *N*, ΔH, ΔS for each experiment.

4.7. Agarose gel electrophoresis studies

Plasmid pUC-19 was linearized with AlwNI at 37 °C for 30 min and the enzyme was heat-inactivated by incubation at 80 °C for 20 min. Linearized pUC-19 was then incubated with varying concentrations of **1a-1f** and **2a-2e**. BamHI was then added and digestion proceeded for 30

min at 37 °C. Samples were then loaded onto a 1% agarose gel containing 0.5 μg/L ethidium bromide and run at 120V for 40 min. A UV transilluminator was used to visualize the gel.

4.8. Molecular docking studies

Compounds **1a**, **1b**, **2d**, and **2e** were minimized in Spartan 14 for Macintosh (Wavefunction, Inc., Irvine, CA). Molecular docking studies were performed with **1a**, **1b**, and **2e** and the Dickerson Drew dodecamer (5′CGCGAATTCGCG-3′) (PDB 436D), and with **2d** and the NFAT sequence (1OWR) using Autodock vina. The search space included both major and minor grooves.

4.9. Electrostatic potential and LUMO maps

Utilizing Spartan 20 for Macintosh (Wavefunction, Inc. Irvine, CA) compound **2d** and the base pairs of 5-GC-3′ were energy minimized (density functional, wB97X-D, 6-31G*) and electrostatic potential maps and HOMO/LUMO maps were generated.

Declaration of Competing Interest

The authors declare that they have no known competing financial interests or personal relationships that could have appeared to influence the work reported in this paper.

Data availability

Data will be made available on request.

Acknowledgments

This paper is dedicated to the memory of Professor Yoshito Kishi. We thank the National Science Foundation, United States (CHE-2003261) and the donors of the American Chemical Society Petroleum Research Fund, United States (62233-UR1) for their generous support of our research program. DC thanks the National Institutes of Health RISE program, United States (GM008395) for support.

Appendix A. Supplementary material

Supplementary data to this article can be found online at https://doi.org/10.1016/j.bmc.2023.117438.

References

[1] (a) Gottesfeld JM, Neely L, Trauger JW, et al., Nature 1997;**387**:202. (b) Leung C-H, Chan DS-H, Ma VP-Y, Ma D-L. Med Res Rev. 2013;**33**:823. (c) Berg T, Curr Opin Chem Biol. 2008;**12**:464.
[2] (a) Hamilton PI, Arya DP. Nat Prod Rep. 2012;**29**:134. (b) Tse WC, Boger DL. Chem Biol. 2004;**11**:1607.
[3] (a) Williams LD, Gao Q. Biochemistry 1992;**31**:4315. (b) Peek ME, Lipscomb LA, Bertrand JA, et al., Biochemistry 1994;**33**:3794. (c) Peek ME, Lipscomb LA, Haseltine J, et al., Bioorg Med Chem. 1995;**3**:693.
[4] (a) Mazzitelli CL, Chu Y, Reczek JJ, et al. J A Soc Mass Spectrom. 2007;**18**:311. (b) Guelev V, Lee J, Ward J, et al., Chem Biol. 2001;**8**:415.
[5] (a) Kumar S, Xue L, Arya DP, J Am Chem Soc. 2011;**133**:7361. (b) B* form DNA refers to AT rich DNA sequences that contain long A tracts leading to an unusually narrow minor groove: N. V. Hud and J. Plavec, Biopolymers 2003;**69**:144.
[6] Bernikova DV, Sosnin NI, Federova OA, Ihmels H. *Org Biomol Chem*. 2018;16:545.
[7] (a) Stefanocci A, Amato J, Brancaccio D, et al., Bioog Chem. 2021;**112**:104836. (b) Stefanucci A, Mosquera J, Vazquez E, et al. A ACS Med Chem Lett. 2015;**6**:1220.
[8] (a) Muller W, Gautier F. Eur J Biochem. 1975;**54**:385. (b) Wakelin LPG, Adams A, Hunter C, et al. Biochemistry 1981;**20**:5779. (c) Chen Y, Wang J, Zhang Y, et al. Photochem Photobiol Sci. 2018;**17**:800. (d) Kim SK, Norden B. FEBS Lett. 1993; **315**:61.
[9] Nunez O, Chavez B, Shaktah R, et al. Bioorg Chem. 2019;**83**:297.
[10] Taber DF, Meagley RP, Supplee DJ. *J Chem Ed*. 1996;73:259.
[11] Barker CC, Bride MH, Stamp A. *J Chem Soc*. 1959:3957.
[12] (a) Morgan AR, Lee JS, Pulleybank, DE, et al., Nucleic Acids Res. 1979;**7**:547. (b) We observed that the fluorescence emission intensity of the CV derivatives above 600 nm (excitation wavelength ~ 550 nm) is minimally altered in the presence of CT DNA; furthermore, the quantum yield of CV in the absence of DNA is 0.019, which is approximately 10-fold lower than that of ethidium bromide (0.15). As a result, ethidium bromide was chosen as the fluorescent reporter for our competition experiments. See: L. A. Brey, G. B. Schuster, H. G. Druckamer, J Chem Phys 1977;**67**:2648.
[13] Sirajuddin M, Ali S, Badshah A. *J PhotoChem Photobiol B: Biol*. 2013;124:1.
[14] (a) Suh D, Chaires JB. Bioorg Med Chem. 1995;**3**:723. (b) Dedon PC, Curr Protoc Nucleic Acid Chem. John Wiley and Sons, New York, 2000, 8.1.1.
[15] (a) White EW, Tanious F, Ismail MA, et al. Biophys Chem. 2007;**126**:140. (b) Triantafillidi K, Karidi K, Malina J, Garoufis A, Dalton Trans. 2009;6403. (c) Hannon MJ, Moreno V, Prieto MJ, et al. Angew Chem Int Ed. 2001;**40**:880.
[16] (a) Garbett NC, Ragazzon PA, Chaires JB. Nat Protoc. 2007;**2**:3166. (b) Monitoring the titration of CT DNA with compound **2b** by CD spectroscopy also provided evidence of minor groove binding (see supporting information), although the competitive inhibition assays indicate lowest affinities for CT DNA in the presence of methyl green.
[17] (a) Lewis EA, Munde M, Wang S, et al. Nucl Acids Res. 2011;**11**:1. (b) Buurma NJ, Haq I. Methods 2007;42:162. (c) Pilch DS, Poklar N, Baird EE, et al. Biochemistry 1999;**38**:2143. (d) Retzeperis D, Dwyer TJ, Geierstanger BH, et al. Biochemistry 1995;**34**:2937. (e) ITC titrations of CT DNA with compound **2b** revealed roughly equivalent enthalpic (ΔH=-3.91±0.08 kcal/mol) and entropic (-TΔS=-4.3 kcal/mol) contributions to the binding free energy.
[18] (a) Chaires JB. Arch Bioch Biophys. 2006;**453**:26. (b) Chaires JB. Biopolymers 1997;**44**:201.
[19] (a) Lukacs CM, Kucera R, Schildkraut I. et al. Nat Struct Biol. 2000;**2**:134. (b) Aggarwal AK. Curr Opin Struct Biol. 1995;**5**:11. (c) Deibert M, Grazulis S, Janulaitis A. et al., EMBO J. 1999;**18**:5805.
[20] Forrow SM, Lee M, Souhami RL. and. *J. A. Hartley Chem. Biol. Interact*. 1995;96: 125.
[21] (a) Tse WC, Boger DL. Acc Chem Res. 2004;**37**:61. (b) Boger DL, Tse WC. Bioorg Med Chem. 2001;**9**:2511.
[22] Stroud JC, Chen L. *J Mol Biol*. 2003;334:1009.
[23] Li J, Rodriguez JP, Niu F, et al. *PNAS*. 2016;113:13015.
[24] Nair SK, Burley SK. *Cell*. 2002;112:193.
[25] Tereshko V, Minasov G, Egli M. *J Am Chem Soc*. 1999;121:470.
[26] (a) Trott O, Olson AJ. J Comput Chem. 2010;**31**:455. (b) The search space included both major and minor grooves as well as the phosphate backbone of DNA. The ligand was first minimized using Spartan 20 for Macintosh (Wavefunction, Inc., Irvine, CA).
[27] Newberry RW, Raines RT. Acc Chem Res. 2017;**50**:1838.
[28] (a) Wang S, Huber PW, Cui M. et al. Biochemistry 1998;**37**:5549. (b) Francois B, Russell RJ, Murray JB, et al., Nucl Acids Res. 2005;**33**:5677. (c) Verhelst SH, Michiels PJ, van der Marel GA. et al. ChemBioChem 2004;**5**:937. (d) Kaul M, Barbieri CM, Pilch DS. J Mol Biol. 2005;**346**:119. (e) Misra VK, Honig B. Proc Natl Acad Sci USA 1995;**92**:4691.
[29] Wilson WD, Tanious FA, Fernandez-Saiz M, Rigl CT. *Methods Mol Biol Drug-DNA Interact Protoc*. 1997;90:219.
[30] (a) Kittler L, Bell A, Baguley BC, Lober G. Biochem Mol Biol Internat. 1996;**40**:263. (b) Forrow SM, Lee M, Souhami RL, Hartley JA. Chemico-Biol Interact. 1995;**96**: 125.
[31] Electrostatic potential maps for **4b** and the base pairs of 5'-GA-3' (energy minimized: density functional, wB97X-D, 6-31G*) were generated by Spartan 20 for Macintosh (Wavefunction Inc, Irvine, CA).
[32] Reinert KE. *J Biomol Struct Dyn*. 1991;9:331.
[33] Urbani M, Torres T. *Chem Eur J*. 2020;26:1683.